Phonon Dispersion Curves of a BC_3 Honeycomb Epitaxial Sheet

H. Yanagisawa,[1,2,*] T. Tanaka,[1,2] Y. Ishida,[1,2] M. Matsue,[1,2] E. Rokuta,[1,2] S. Otani,[3] and C. Oshima[1,2]

[1]*Department of Applied Physics, Waseda University, 3-4-1 Okubo, Shinjuku-ku Tokyo 169-8555, Japan*
[2]*Kagami Memorial Laboratory for Material Science and Technology, Waseda University,*
2-8-26, Nishiwaseda, Shinjuku-ku, Tokyo 169-0051, Japan
[3]*National Institute for Material Science, 1-1, Namiki, Tsukuba-shi, Ibaraki 305-0044, Japan*

(Received 12 November 2003; published 18 October 2004)

The entire phonon-dispersion curves along the $\overline{\Gamma}$-$\overline{\mathrm{M}}$ direction of a BC_3 honeycomb sheet have been determined both experimentally and theoretically for the first time. Most of the observed curves agreed with the theoretical ones calculated on the basis of *ab initio* theory. From the stretching force constants of the nearest-neighbor C-C and B-C bonds, together with that of the B-B bond, we clarified the characteristic feature of the C-C and B-C bonds. From the experimental and theoretical results, we discussed the possibility of high T_c.

DOI: 10.1103/PhysRevLett.93.177003 PACS numbers: 74.70.Dd, 63.20.Dj, 68.35.Ja, 82.80.Pv

Recently, a new group of graphitic materials constituted by boron, carbon, and nitrogen has intrigued fundamental explorations in material science, because of its peculiar atomic structure and its characteristic physical properties. For instance, they are fullerenes [1], nanotube [2], *hexagonal* boron nitride (*h*-BN) [3,4]. In particular, boron-carbon honeycomb structures such as BC and BC_3 [5] were investigated theoretically in relation to high superconducting transition temperatures (T_c) of LiBC [6] and Mg_2BC_3 [7], being isomorphic of MgB_2 ($T_c =$ 39 K) [8]. Nevertheless, no macroscopic single crystals of those materials were available so far, and experimentally; hence little was confirmed about those interesting calculations concerning phonon structures, electronic energy bands, and T_c.

In our other paper, we reported the growth of a uniform BC_3 honeycomb sheet with excellent crystalline quality over a macroscopic surface area of $NbB_2(0001)$ [9]. All the observed data on the chemical compositions, lattice constants, low-energy electron diffraction (LEED) intensity distribution, and electronic band structures indicated clearly that the uniform BC_3 honeycomb sheet was grown in the epitaxial way on the substrate. This is the first macroscopic uniform film of a single-crystal BC_3 sheet with a monolayer thickness. In the present work, we have determined experimentally the phonon-dispersion curves of this BC_3 honeycomb sheet along the $\overline{\Gamma}$-$\overline{\mathrm{M}}$ direction and compared them with theoretical curves calculated on the basis of the *ab initio* theory. In the analysis of the data, these results reveal the bonding manner in a BC_3 layer and would provide us prominent knowledge about the phonons in a high T_c superconductor.

The experiments were carried out in an ultrahigh vacuum chamber equipped with a cylindrical mirror analyzer for Auger-electron spectroscopy, LEED optics, and a high-resolution electron-energy-loss spectrometer (HREELS) for measurement of phonon-dispersion curves. Both the BC_3 and graphite layers were grown in the epitaxial way on the $NbB_2(0001)$ substrate, as we reported in our other paper [9]. In the LEED pattern, we observed sharp diffraction spots indicative of either a BC_3 or a graphite layer, each of which was clearly distinguishable from the other owing to the distinct difference in the lattice constant.

The theoretical phonon-dispersion curves were obtained on the basis of an *ab initio* calculation (DACAPO package [10]). Plane-wave functions with the cutoff energy at 36.7 Ry were used as the basis set and a generalized gradient approximation [11] for the exchange-correlation potential. The fundamental procedure to calculate the phonon-dispersion curves was the same as that proposed by Kunc *et al.* [12], in which the dynamical-matrix elements were evaluated from the Hellmann-Feynman forces generated by a slight displacement of the linearly chained atoms [13]. In the calculation of the lattice dynamics, we employed the atomic arrangement in the BC_3 sheet depicted schematically in Fig. 1, which was verified to yield the highest cohesive energy among the possible structures with the same chemical composition [14]. The atomic positions were optimized

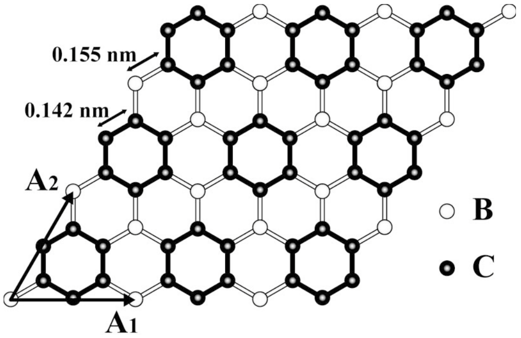

FIG. 1. A schematic representation of the BC_3 atomic structure with the highest cohesive energy among those with the same concentration.

by the iterative loops of the calculation, and the result proved to be identical to that of the previous study [15]; the C-C and B-C bond lengths were 0.142 and 0.155 nm, respectively. The calculated lattice constant, 0.52 nm, was in perfect agreement with the one yielded by LEED, 0.52 ± 0.02 nm.

Prior to the investigation into the BC_3 honeycomb sheet, we measured the phonon-dispersion curves of graphite layers grown on the previously mentioned NbB_2 substrate to ensure the reliability of our experimental techniques and *ab initio* calculations. We compared these curves with both the theoretical calculations and the previous experimental data on bulk graphite [16]. Figure 2 represents the results. The solid and open circles depict the data points of the graphite layer and bulk graphite, respectively, and the solid lines indicate the theoretical dispersion curves of a graphene sheet. As shown in Fig. 2, the three kinds of the data of the graphite phonons are in almost perfect agreement with each datum. The only exception was the difference in the transverse acoustic (TA) mode. Specifically, in this mode, no data points appeared for the graphite layer, while the TA curves were detected in the bulk graphite. The HREELS selection rule states that the TA mode along the $\overline{\Gamma}$-$\overline{M}$ direction should be unobservable owing to the reflectional symmetry [17]. Hence, the contrasting results suggest that the crystalline quality of the graphite layers was higher than that of the bulk crystal. This tendency is consistent with the findings regarding the LEED spots; the diffraction spots of the graphite layer on $NbB_2(0001)$ were much sharper than those of the bulk graphite. Thus, the above data indicated that both the experimental measurements and the theoretical calculations ensure the reliability in the investigation of the isostructural BC_3 honeycomb sheet.

Figure 3 shows the HREEL spectra of the $BC_3/NbB_2(0001)$ for the various wave vectors along the $\overline{\Gamma}$-$\overline{M}$ direction in the two-dimensional surface Brillouin zone, which is depicted in Fig. 4. As denoted by the triangles in Fig. 3, at least seven loss peaks were recognizable in isolation in each spectrum; this is a larger number than were found in the graphite-layer spectra [16,18]. The large number clearly indicates that the unit cell of the BC_3 is larger than that of the graphite layer.

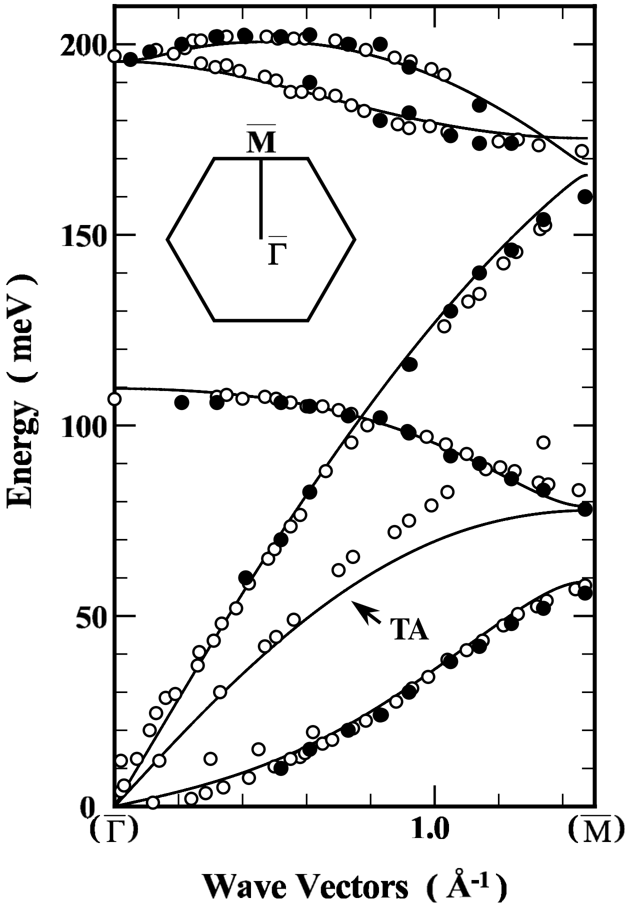

FIG. 2. Phonon energy dispersion curves of graphite. Experimental data of monolayer graphite films on $NbB_2(0001)$ (solid circles) and bulk graphite (open circles) are compared with an *ab initio* calculation (solid lines).

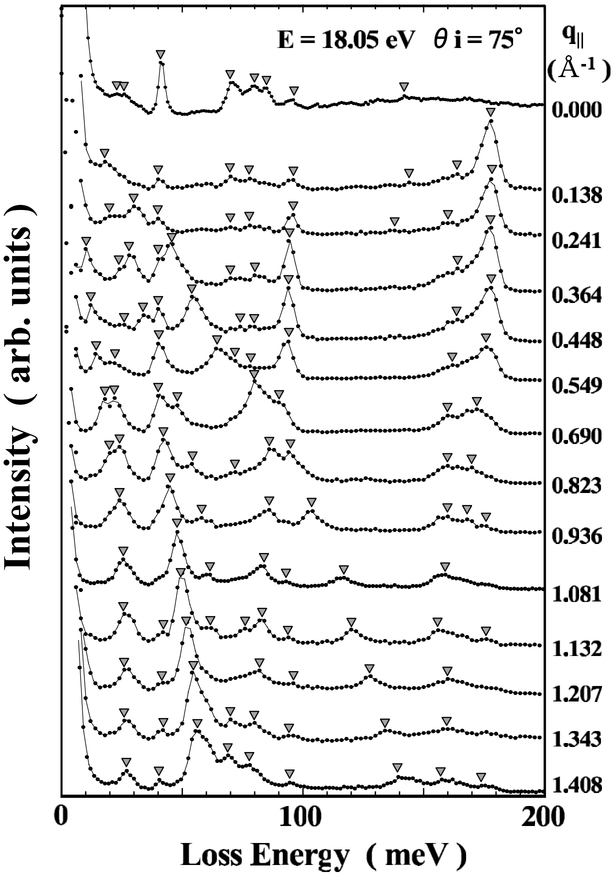

FIG. 3. HREEL spectra of monolayer BC_3 films on $NbB_2(0001)$ as a function of wave vectors. Energy loss peaks are noticed by triangles, and the scanned direction is pictorially indicated in the depicted surface Brillouin zone.

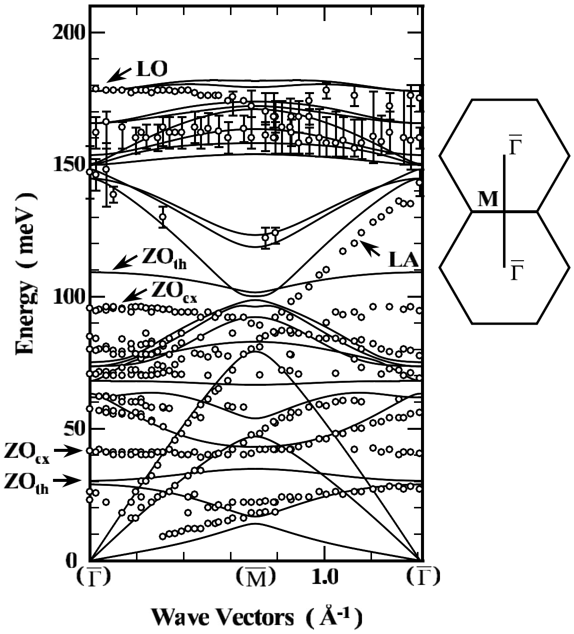

FIG. 4. Experimentally determined phonon energy dispersion curves of honeycomb BC_3 sheet (open circles), and theoretical curves obtained based on the *ab initio* calculation. Some characteristic branches are denoted by capital letters; see the text.

Regarding the phonon energy, on the other hand, high frequency phonon optical bands ranging from 150 to 180 meV were clearly detected for all the wave vectors. The highest-frequency phonons were located beyond the maximum energies of the phonons in the boron-honeycomb layers in some metal diborides, about 90 meV [19,20], and slightly below those of graphite, about 200 meV [16]. Accordingly, the Debye temperature of the BC_3 sheet is intermediate between those of the graphite and boron-honeycomb layers.

By plotting the energies of the loss peaks in the HREEL spectra against the wave vectors, we determined the phonon energy dispersion curves of the BC_3 sheet as shown in Fig. 4. The open circles represent the experimental data points and the solid lines represent the theoretical curves. The longitudinal acoustic (LA) branch appeared in the wide energy region, and the large dispersion curve of the LA phonons is a characteristic feature of the materials with high vibrational energies.

All the experimental curves except the ZO and ZO$'$ phonons are explicable on the basis of the *ab initio* dynamics. The vibrational energies of the ZO phonons with out-of-plane polarization were about 10 meV lower than the theoretical ones. A similar softening of the ZO phonons was seen in both monolayer films of graphene and hexagonal boron nitride on various surfaces [4,18]. The phenomenon is related to an orbital hybridization between the π band of the honeycomb layers and the d band of the substrate [3,21]. The out-of-plane π bands of the BC_3 film presumably hybridize with the substrate electronic states. The stiffening of ZO$'$ phonons in Fig. 4 is presumably attributed to the same orbital hybridization. In contrast, the other experimental data points were reproduced by the *ab initio* lattice dynamics.

From the dynamical matrix which determines the phonon-dispersion curves in Figs. 2 and 4, we retrieved stretching force constants (FCs) of the nearest-neighbor bonds. Here, $F_{X\text{-}Y}$ means the FC of the nearest-neighbor X-Y bond, and X and Y stand for either carbon or boron atoms. Table I shows a list of $F_{X\text{-}Y}$ of the nearest-neighbor C-C, B-C, and B-B bonds. The FC changes as follows: $F_{\text{C-C}} > F_{\text{B-C}} \gg F_{\text{BB}}$. In the BC_3 sheet, $F_{\text{B-C}}$ is three-fourths of $F_{\text{C-C}}$, while $F_{\text{B-B}}$ is about one-fourth of $F_{\text{C-C}}$. On the other hand, it should be remarked that the $F_{\text{C-C}}$ of BC_3 is the same as that of graphite, which means that the binding energies of the C-C bonds are also the same. The similar relation was found in the list of the bond lengths shown in Table I: The C-C bond length in the BC_3 sheet is the same as that in graphite. In addition, the changes in the other bond lengths are consistent with the changes in the corresponding FCs. With increasing the bond length, the FC decreases.

Concerning the superconducting states, the dominant parameter for realization of high T_c is electron-phonon coupling [22]. In the earlier stage of the growth process used in this experiment, recently, we succeeded to grow a metastable BC_3 (m-BC_3) sheet with large lattice constant and soft phonons as compared with those of the stable BC_3 sheet discussed above. With successive heatings at 1300 °C, the m-BC_3 sheet is changed irreversibly to the stable BC_3 sheet. Owing to the interaction with the substrate Nb atoms, the atoms in the m-BC_3 sheet are forced to align in the commensurate manner. As a result, the atomic distances are longer than that of the incommensurate BC_3 sheet by 0.02 nm. The dispersion curves of the LO phonons appeared around 160 meV, which is about 20 meV lower than that of the incommensurate sheet in

TABLE I. A list of stretching force constants (FCs) of the nearest-neighbor bonds in graphite, BC_3 and NbB_2. The FCs of the C-C and B-C bonds based on the *ab initio* calculations in the first column produce dispersion curves in Figs. 2 and 4. The FCs of the B-B and C-C bonds in the second column are determined as the fitting parameters in the force constant model [18,20]. Atomic distances of those bonds are also shown.

	Ab initio FCs (10^4 dyn/cm)	Fitting FCs (10^4 dyn/cm)	Bond length (nm)
$F_{\text{C-C}}$ (graphite)	41.6	36.4[a]	0.142[a]
$F_{\text{C-C}}$ (BC_3)	41.0		0.142[b]
$F_{\text{B-C}}$ (BC_3)	29.4		0.155[b]
$F_{\text{B-B}}$ (NbB_2)		8.8[c]	0.180[c]

[a] Reference [18].
[b] Reference [15].
[c] Reference [20].

Fig. 4. If we assumed that the observed energy shifts originate from the hole-doping effects predicted in a recent paper [23], we can expect a large enhancement of electron-phonon coupling, resulting in high T_c [24]. Hence, the BC_3 honeycomb sheets are promising materials for the realization of high T_c, because of their large freedom of interaction with the substrate to increase the electron-phonon coupling.

In summary, the entire phonon-dispersion curves of a BC_3 honeycomb sheet have been determined both experimentally and theoretically. The experimental curves are in good accordance with the *ab initio* results. From those data, the FCs of three different bonds are clarified quantitatively, and the possibility of high T_c is discussed.

We acknowledge many useful discussions with Dr. T. Kimura. This work was supported in part by JSPS and the Ministry of Education, Sports, Culture, Science and Technology as the research for the future program of development of ultracoherent electron beam, and by a Grant-in-Aid for The 21st Century COE Program (Physics of Self-organization Systems) at Waseda University from the Ministry of Education, Sports, Culture, Science and Technology

---

*Electronic address: hyanagisawa@ruri.waseda.jp

[1] H.W. Kroto, J. R. Heath, S. C. O'Brien, and R. E. Smally, Nature (London) **318**, 162 (1985).
[2] S. Iijima, Nature (London) **354**, 56 (1991).
[3] A. Nagashima, N. Tejima, Y. Gamou, T. Kawai, and C. Oshima, Phys. Rev. Lett. **75**, 3918 (1995).
[4] E. Rokuta, Y. Hasegawa, K. Suzuki, Y. Gamou, C. Oshima, and A. Nagashima, Phys. Rev. Lett. **79**, 4609 (1997).
[5] J. Kouvetakis, R. B. Kaner, M. L. Sattler, and N. Bartlett, J. Chem. Soc. Chem. Commun. **1986**, 1758 (1986).
[6] H. Rosner, A. Kitaigorodsky, and W. E. Pickett, Phys. Rev. Lett. **88**, 127001 (2002).
[7] R. A. Jishi, M. Benkraouda, and J. Bragin, Phys. Lett. A **306**, 358 (2003).
[8] J. Nagamatsu, N. Nakagawa, T. Muranaka, Y. Zenitani, and J. Akimitsu, Nature (London) **410**, 63 (2001); R. M. Wentzcovitch, M. L. Cohen, S. G. Louie, and D. Tomanek, Solid State Commun. **67**, 515 (1988).
[9] H. Tanaka, Y. Kawamata, H. Shimizu, T. Fujita, H. Yanagisawa, S. Otani and C. Oshima (to be published).
[10] The software package has been provided by the CAMP project and is accessible at http://www.fysik.dtu.dk
[11] J. P. Perdew, J. A. Chevary, S. H. Vosko, Koblar A. Jackson, Mark R. Pederson, D. J. Singh, and Carlos Fiolhais, Phys. Rev. B **46**, 6671 (1992).
[12] K. Kunc and R. M. Martin, Phys. Rev. Lett. **48**, 406 (1982); K. Kunc and P. G. Dacosta, Phys. Rev. B **32**, 2010 (1985).
[13] In our analyses, various atomic displacements ranging from 0.0005 to 0.002 nm were examined. We found that the calculated results were independent on the displacement in this range.
[14] Q. Wang, L.-Q. Chen, and J. F. Annett, Phys. Rev. B **54**, R2271 (1996).
[15] D. Tomanek, R. M. Wentzcovitch, S. G. Louie, and M. L. Cohen, Phys. Rev. B **37**, 3134 (1988).
[16] C. Oshima, T. Aizawa, R. Souda, Y. Ishizawa, and Y. Sumiyoshi, Solid State Commun. **65**, 1601 (1988).
[17] H. Ibach and D. L. Mills, *Electron Energy Loss Spectroscopy and Surface Vibrations* (Academic, New York, 1982).
[18] T. Aizawa, R. Souda, S. Otani, Y. Ishizawa, and C. Oshima, Phys. Rev. B **42**, 11469 (1990).
[19] K.-P. Bohnen, R. Heid, and B. Renker, Phys. Rev. Lett. **86**, 5771 (2001).
[20] T. Aizawa, W. Hayami, and S. Otani, Phys. Rev. B **65**, 024303 (2001).
[21] A. Nagashima, K. Nuka, H. Itoh, T. Ichinokawa, S. Otani, and C. Oshima, Surf. Sci. **291**, 93 (1993).
[22] W. L. McMillan, Phys. Rev. **167**, 331 (1968).
[23] F. J. Ribeiro, and M. L. Cohen, Phys. Rev. B **69**, 212507 (2004).
[24] $T_c = 20$ K is estimated for the m-BC_3 sheet by using the result of Ref. [23]. The observed energy shift of 20 meV corresponds to the hole doping of 0.15 holes/cell, which enhances electron-phonon coupling by a factor of 20.